International Journal of Mechanical, Industrial and Aerospace Sciences
ISSN: 2517-9950
Vol:9, No:7, 2015

Numerical and Experimental Studies of Joule Heating Effects around Crack and Notch Tips

Thomas Jin-Chee Liu, Ji-Fu Tseng, Yu-Shen Chen

***Abstract*—**This paper investigates the thermo-electric effects around the crack and notch tips under the electric current load. The research methods include the finite element analysis and thermal imaging experiment. The finite element solutions show that the electric current density field concentrates at the crack tip. Due to the Joule heating, this electric concentration causes the hot spot at the tip zone. From numerical and experimental results, this hot spot is identified. The temperature of the hot spot is affected by the electric load, operation time and geometry of the sample.

***Keywords*—**Thermo-electric, Joule heating, crack tip, notch tip.

I. Introduction

MANY researches have reported that the Joule heating effect can induce the local hot spot or melting area at the crack tip [1]-[8]. This phenomenon is a kind of the thermo-electric effect. As shown in Fig. 1, when the crack tip is subjected to the electric load, the electric current density field concentrates at the crack tip. Due to the Joule heating, the electric concentration causes the hot spot at the crack tip zone.

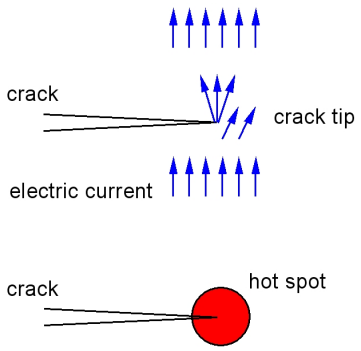

Fig. 1 Hot spot at crack tip

In the past studies [1]-[8], the results demonstrated that the crack tip can melt when large electric energy is applied. After the cooling process, the melting area can become a hole at the crack tip. This hole, like a drilled hole, can reduce the stress concentration and remove the stress singularity at the crack tip. It can prevent from the further crack growth. If the applied electric energy is lower and sufficient, the local hot spot exists at the crack tip. This phenomenon can be applied on the thermal sensing technique for detecting cracks or fractures in metal components [4].

This paper investigates the thermo-electric effects around the crack and notch tips under the electric current load. The research methods include the finite element analysis and thermal imaging experiment. The temperature of the hot spot at the tip zone is discussed. The effects of the electric load, operation time and geometry of the sample are investigated. Finally, the industrial applications of this research will be proposed.

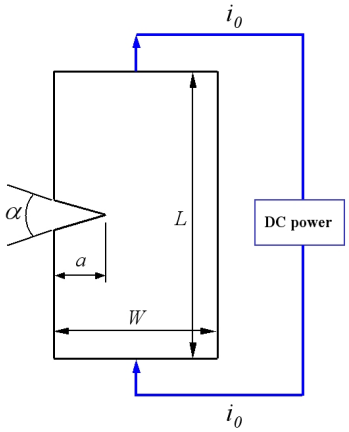

Fig. 2 Sample geometry of this research

II. Problem Definition

In Fig. 2, it shows the sample geometry and electric load of this research. The thin plate has the dimensions $W \times L$ and thickness e. The crack or notch length is denoted as a. The notch angle is α. The sample is subjected to a direct current (DC) i_0. The material type of the sample is the SUS 304 stainless steel. Table I lists the material data of the SUS 304 stainless steel [9]. The thermal conductivity and electric resistivity are temperature-dependent.

The following conditions are considered in this study:

(1) Three-dimensional analysis
(2) Thermo-electric coupled-field
(3) Transient heat transfer
(4) Convection on air/sample interface
(5) Steady electric current (DC current)
(6) Temperature-dependent material data

Thomas Jin-Chee Liu, Associate Professor, is with the Department of Mechanical Engineering, Ming Chi University of Technology, Taishan, New Taipei City, Taiwan. (corresponding author to provide phone: 886-2-29089899 ext 4569; e-mail: jinchee@mail.mcut.edu.tw).

Ji-Fu Tseng is an undergraduate student in the Department of Mechanical Engineering, Ming Chi University of Technology.

Yu-Shen Chen was a graduate student in the Graduate Institute of Electro-Mechanical Engineering, Ming Chi University of Technology.

(7) Electric insulation on crack surface

TABLE I
MATERIAL DATA OF SUS 304 STEEL [9]

Density, kg/m^3	8000
Thermal conductivity, W/(m-°C)	16.2 @ 0~100 °C 21.5 @ 500 °C
Specific heat, J/ (kg-°C)	500
Resistivity, Ω-m	7.2×10^{-7} @ 20 °C 7.8×10^{-7} @ 100 °C 8.6×10^{-7} @ 200 °C 10×10^{-7} @ 400 °C 11.6×10^{-7} @ 650 °C

III. BASIC THEORY

In this study, the basic theory of the thermo-electric coupled-field analysis is described by the following equations [10]-[12]:

$$\mathbf{E} = -\nabla\phi \ , \ \mathbf{J} = \frac{1}{\rho}\mathbf{E} \ , \ \nabla\cdot\mathbf{J} = 0 \tag{1}$$

$$\mathbf{q}'' = -k\nabla T \ , \ k\nabla^2 T + \dot{q} = \beta C_p \frac{\partial T}{\partial t} \ , \ \dot{q} = \rho|\mathbf{J}|^2 \tag{2}$$

$$\begin{bmatrix} \mathbf{C}^t & 0 \\ 0 & 0 \end{bmatrix}\begin{Bmatrix} \dot{\mathbf{T}} \\ \dot{\mathbf{V}} \end{Bmatrix} + \begin{bmatrix} \mathbf{K}^t & 0 \\ 0 & \mathbf{K}^v \end{bmatrix}\begin{Bmatrix} \mathbf{T} \\ \mathbf{V} \end{Bmatrix} = \begin{Bmatrix} \mathbf{Q} \\ \mathbf{I} \end{Bmatrix} \tag{3}$$

In (1), **E**, **J**, ϕ and ρ are the electric field, electric current density, electric potential and resistivity, respectively. In (2), $\mathbf{q}''$, k, T, $\dot{q}$, β, C_p and t are the heat flux, thermal conductivity, temperature, heat generation of Joule heating, mass density, specific heat and time, respectively. In (3), **T**, **V**, **Q** and **I** are the vector forms of the temperature, electric potential, heat flow rate and electric current, respectively. The material constant matrices $\mathbf{C}^t$, $\mathbf{K}^t$ and $\mathbf{K}^v$ are the thermal specific heat, thermal conductivity and electric conductivity, respectively. The coupled heat flow matrix **Q** contains the effects of the thermal loading and electrical Joule heating. Equation (3) is a directly coupled nonlinear equation which is solved using the Newton-Raphson iterative method. Equations (1)–(3) will be solved using the finite element software ANSYS [12].

IV. FINITE ELEMENT METHOD

Fig. 3 shows the finite element model of ANSYS with the dimensions: W=10 mm, L=240 mm, e=0.05 mm, a=5 mm and α=0°. It is modeled by the SOLID226 element, i.e. the 20-node isoparametric solid element associated with the thermo- electric analysis. The crack tip region is modeled by the quarter-point elements for expressing the $r^{-1/2}$ singularity of the electric current density field. This model contains 2824 elements.

V. EXPERIMENTAL METHOD

Fig. 4 shows the experimental facilities of this study. The SUS 304 steel sample is connected to the DC power supplier. Due to the Joule heating effect, the sample is heated. The thermal image camera (designed by FLIR Co.) is used to capture the surface temperature field of the sample. The sample is a steel strip as shown in Fig. 5. It has an edge crack in the central region. To capture the surface temperature image, the sample must be coated by the black paint.

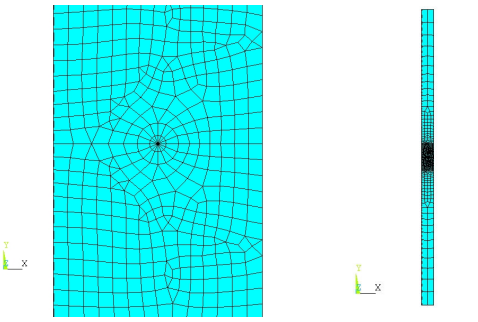

(crack region) (full model)

Fig. 3 Finite element model

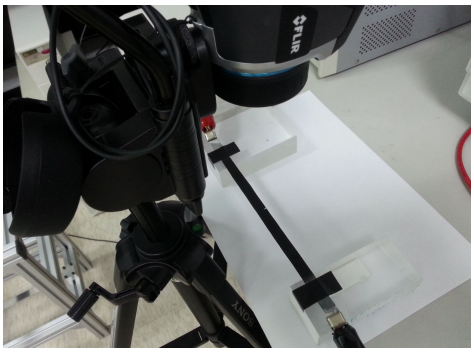

Fig. 4 Experimental facilities

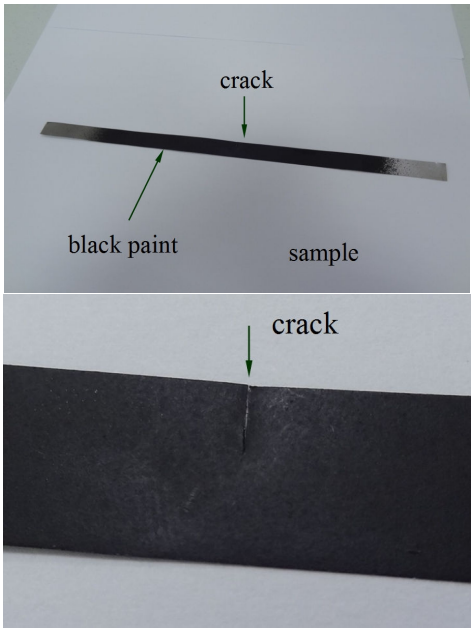

Fig. 5 Sample

VI. Results and Discussions

A. Finite Element Results

The finite element model as shown in Fig. 3 uses the coupled-field analysis. The initial and ambient temperature are 26°C. The natural convection coefficients applied on the strip surfaces are calculated from the simplified formula in Ref. [13]. As a result, Figs. 6 and 7 show the electric current density and temperature field under $i_0 = 5$ A at 60 s. It can be seen that the Joule heating effect causes a high temperature area (hot spot) around the crack tip. Also, there is a local concentration of the electric current density near the crack tip. Similar to the elastic stress field, the electric current density also has the $r^{-1/2}$ singularity at the crack tip [2].

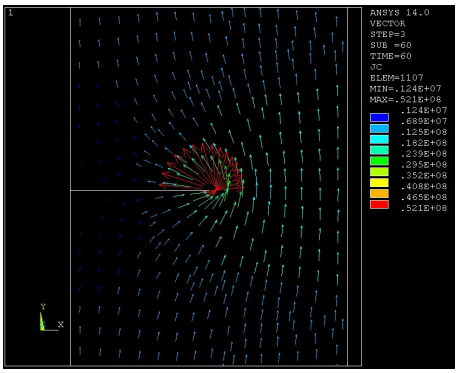

Fig. 6 Electric current density vectors (A/m^2)

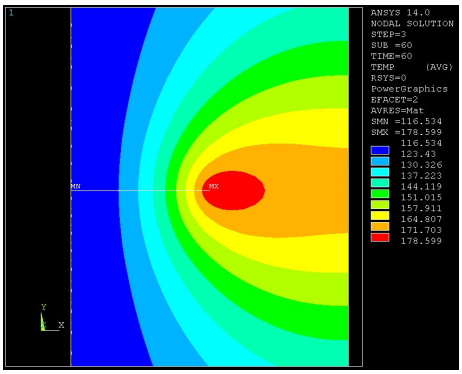

Fig. 7 Temperature contour (ºC)

B. Comparison of Two Methods

In this experimental study, the sample geometry and all conditions are the same as the finite element model in Section VI *A*. Fig. 8 shows the thermal image of the steel strip with a crack. There is a local hot spot around the crack tip.

The crack tip temperatures with time increments are shown in Fig. 9. The finite element results (numerical results) are close to experimental results. It demonstrates the good prediction of the numerical simulation.

C. Effects of Geometry and Electric Load

In the experiments of this section, effects of the sample geometry and electric load are discussed. In Fig. 10, the time-history data of the crack tip temperature are shown with different sample thickness. Due to the current density, the thinner case has higher temperature.

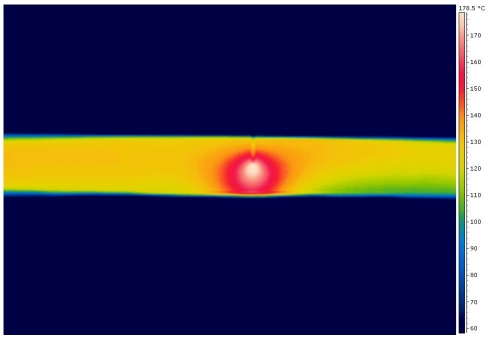

Fig. 8 Thermal image (ºC) ($i_0 = 5$ A at 60 s)

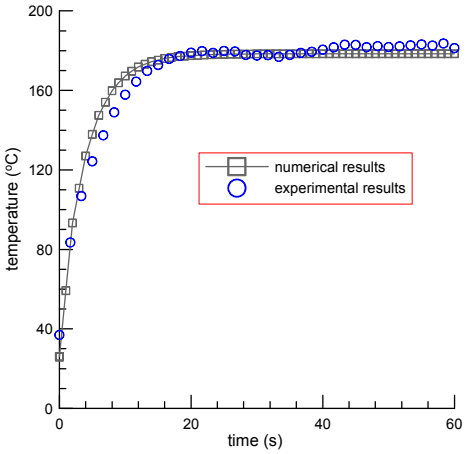

Fig. 9 Time-history results

For the fixed geometry and operation time, the magnitude of the electric load affects the crack tip temperature. In Fig. 11, higher electric load causes higher temperature field on the steel strip. In addition, Fig. 12 shows the thermal image under $i_0 = 4$ A at 120 s.

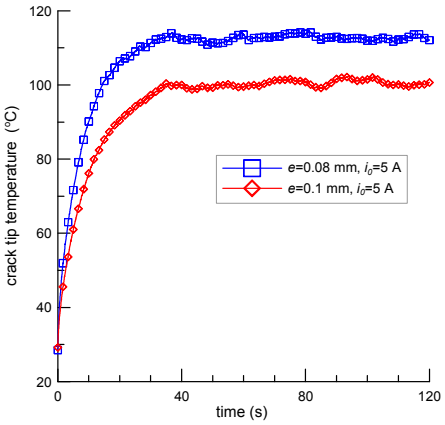

Fig. 10 Time-history results

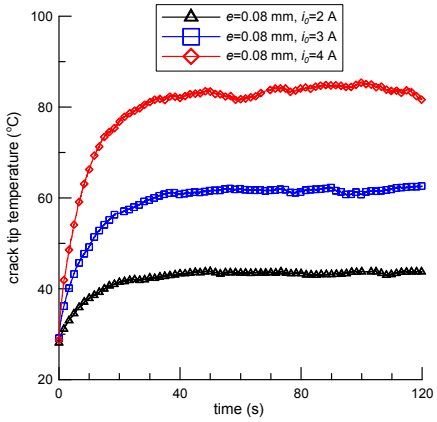

Fig. 11 Time-history results

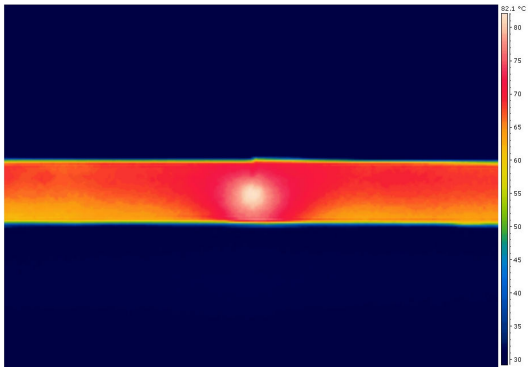

Fig. 12 Thermal image (ºC) (e=0.08 mm, i_0 = 4 A, 120 s)

D. Notch Study

In this section, the sample is a steel strip with a sharp notch. The dimensions are W=10 mm, L=240 mm, e=0.05 mm, a=5 mm and α=5°. The electric load is i_0 = 5 A. Fig. 13 shows the thermal image at 60 s. There is also a hot spot near the notch tip.

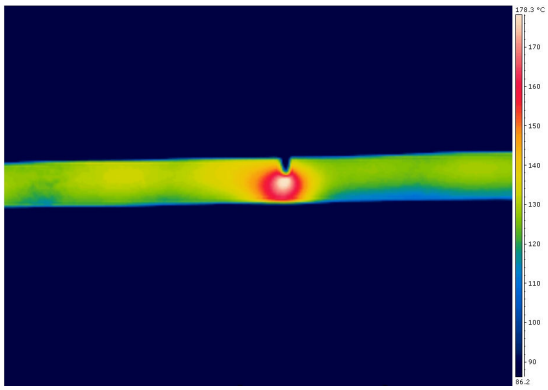

Fig. 13 Thermal image (ºC) (α=5°)

VII. Conclusions

According to numerical and experimental results, the hot spot around the crack tip or notch tip is identified. The temperature of the hot spot is affected by the electric load, operation time and geometry of the sample.

The concept and result of this research can be applied to the crack detection. Using the thermal camera and image, the crack tip location can be determined. On the other hand, this research can be applied to the crack arrest. Under the high electric energy, the crack tip can melt and shrink to a hole. The crack tip hole can arrest or stop the further crack propagation.

Acknowledgments

The authors would like to thank the Ministry of Science and Technology in Taiwan for the financial support under contract numbers NSC 101-2221-E-131-011 and MOST 103-2221-E-131-015. Also, the authors appreciate the support of the research project 103-AcademicResearch- E-02 of Ming Chi University of Technology.

References

[1] Parton VZ and Kudryavtsev BA. *Electromagnetoelasticity*. Gordon and Breach, New York, 1988.
[2] Cai GX and Yuan FG. Electric current-induced stresses at the crack tip in conductors. *Int. J. Fract.* 96, pp. 279–301, 1999.
[3] Fu YM, Bai XZ, Qiao GY, Hu YD and Luan JY. Technique for producing crack arrest by electromagnetic heating. *Mater. Sci. Tech.* 17, pp. 1653–1656, 2001.
[4] Hasanyan D, Librescu L, Qin Z and Young RD. Thermoelastic cracked plates carrying nonstationary electrical current. *J. Therm. Stress.* 28, pp. 729–745, 2005.
[5] Qin Z, Librescu L and Hasanyan D. Joule heating and its implications on crack detection/arrest in electrically conductive circular cylindrical shells. *J. Therm. Stress.* 30, pp. 623−637, 2007.
[6] Liu TJC. Finite element modeling of melting crack tip under thermo-electric Joule heating. *Engng. Fract. Mech.* 78, pp. 666−684, 2011.
[7] Liu TJC, Joule heating behaviors around through crack emanating from circular hole under electric load, *Engng. Fract. Mech.* 123, pp. 2-20, 2014.
[8] Liu TJC, Crack detection/arrest with Joule heating. *Encyclopedia of Thermal Stresses*, Hetnarski, R.B. (Ed.), Springer Science + Business Media Dordrecht, Dordrecht, 2013.
[9] Online Materials Information Resource – *MatWeb*, http://matweb.com/
[10] Cheng DK, *Field and Wave Electromagnetics*, Addison-Wesley, MA, 1983.
[11] Incropera FP and DeWitt DP, *Fundamentals of Heat and Mass Transfer*, Fifth Ed., John Wiley & Sons, USA, 2002.
[12] *ANSYS HTML Online Documentation*, SAS IP, Inc., USA, 2005.
[13] McAdams WH, *Heat Transmission*, 3rd Ed., McGraw-Hill, New York, 1954.